Research Square

Preprints are preliminary reports that have not undergone peer review.
They should not be considered conclusive, used to inform clinical practice,
or referenced by the media as validated information.

Distinct subthalamic and pallidal beta dynamics in Parkinson's disease

Valentina D'Onofrio
University of Padua
Gerd Tinkhauser
Bern University Hospital and University of Bern
Dario Ciprietti
University of Padua
Laura Ludovica Grassi
University of Padua
Sofia Pavan
University of Padua
Elena Bernasconi
Bern University Hospital and University of Bern
Alberto Averna
Bern University Hospital and University of Bern
Andrea Landi
University of Padua
Camillo Porcaro
University of Padua
Angelo Antonini
University of Padua
Andrea Guerra
andrea.guerra@unipd.it
University of Padua

Article

Keywords:

Posted Date: March 8th, 2026

DOI: https://doi.org/10.21203/rs.3.rs-8976619/v1

License: This work is licensed under a Creative Commons Attribution 4.0 International License. Read Full License

Additional Declarations: Competing interest reported. The authors declare the following competing interests: G.T. received financial support from Boston Scientific and Medtronic, not related to the present work. G.T., A.Av. and E.B. receive funding from the Swiss National Science Foundation (project number: PZ00P3_202166), not related to the present work. G.T. and A.Av. received funding from the Swiss Parkinson Association. A.A. has received honoraria/consultation fees from AbbVie, Bial, Bayer, Stada, Covantec, Ever Pharma, Medscape, Roche, Theravance Biopharma, UCB, and Zambon, , not related to the present work. A.A. has also received funding from Horizon 2020 - Ministry of University and Research (MIR), Ministry of Health (MOH), European Union - NextGenerationEU – NRRP M6C2 - Investment: 2.1 "Enhancement and strengthening of biomedical research within the NSH", not related to the present work. A.G. has received compensation for consultancy and speaker-related activities from Bial, Zambon, STADA; he receives funding from the European Union "Next Generation EU, Mission 4 Component 1, Project code: P20223HHZ8, CUP: C53D23008440001", not related to the present work.

Abstract

Despite the clinical use as a Deep Brain Stimulation (DBS) target in Parkinson's disease (PD) and recent approval for adaptive stimulation, beta dynamics in the Globus Pallidus internus (GPi) remain poorly defined compared to the Subthalamic Nucleus (STN). We investigated target-specific beta activity in Local Field Potentials recorded in PD patients implanted with sensing-enabled STN- or GPi-DBS and examined differential modulation by L-Dopa and stimulation and relationship with motor symptoms. In the untreated state, spectral profiles were comparable between targets. L-Dopa selectively reduced low-beta power and burst durations in the STN, while suppressing high-beta activity in the GPi. DBS induced broadband beta suppression and burst shortening in the STN, whereas attenuated pallidal high-beta oscillations. Clinical improvement correlated with low-beta modulation in STN patients and high-beta modulation in GPi patients. Low- and high-beta sub-bands exhibit distinct target-specific pathophysiological behaviour and responsiveness. These findings provide a physiological framework for frequency-tailored adaptive DBS.

Introduction

The Subthalamic Nucleus (STN) and the Globus Pallidus internus (GPi) are well-established deep brain stimulation (DBS) targets in Parkinson's disease (PD)[1–3]. Despite comparable efficacy in motor symptoms improvement, many studies suggest that stimulation of these two nuclei may differ in several clinically relevant aspects, including stimulation sensitivity, postoperative management of dopaminergic therapy and ultimately in patient profile selection[4–8]. However, the neurophysiological mechanisms underlying these differences remain poorly understood. While STN and GPi are embedded within the same cortico–basal ganglia circuits and share several direct and indirect projections, they differ substantially in neuronal populations, neurotransmitter systems, as well as local and long-range synaptic connections[9–11]. These distinctions likely underlie divergent neurophysiological properties and differential responses to therapeutic interventions (i.e., L-Dopa and DBS).

Pathologically enhanced activity in the beta frequency band (13–30 Hz) within the STN represents a robust neurophysiological hallmark of PD[12–15], as abnormal beta oscillations are typically suppressed by both DBS and L-Dopa and are closely related to motor impairment[16–20]. Notably, beta activity across its entire spectral range is not uniform, since low-beta oscillations (13–20 Hz) have been more directly linked to motor impairment, whereas high-beta activity (20–30 Hz) has been related to long-range cortico-basal communication[21–24]. Additionally, beta oscillations occur in transient bursts, whose duration and amplitude are modulated by L-Dopa[20,25,26] and DBS[27–30]. This evolving understanding of beta dynamics in the STN has translated into clinical optimisation of many aspects of DBS therapy, including closed-loop adaptive DBS (aDBS) and neurophysiologically-assisted DBS programming[15,31–34].

Conversely, neurophysiological dynamics in the GPi remain far less explored. The limited available studies exploring pallidal neurophysiological dynamics in PD have reported exaggerated beta-band activity[35–39]. Importantly, all previous studies were performed during surgery or in the early postoperative period, with many aiming to assess differences between PD and other movement disorders, such as dystonia and Tourette syndrome[39–41]. Only two studies directly compared neurophysiological features of GPi and STN, though in small PD patient cohorts[35,36], while a systematic comparative assessment of the combined effects of L-Dopa and DBS is lacking. Understanding the spectral properties and behaviour of these common DBS targets is of pathophysiological interest and crucial to validate biomarkers for optimal use of sensing-guided DBS in clinical practice.

In the present study, we investigated and directly compared beta activity in PD patients chronically treated with STN- or GPi-DBS and its modulation by L-Dopa, DBS, and their combination. To unravel target-specific beta dynamics characterising the intrinsic properties of the two nuclei, we comprehensively assessed beta power spectrum, peak amplitude, and burst characteristics under different therapeutic conditions. Finally, to assess whether neurophysiological differences are relevant in motor symptom pathophysiology, possible correlations with motor symptoms were tested.

Results

Demographic and clinical characteristics

The STN- and GPi-DBS patient cohorts were comparable in gender distribution, age, disease duration at surgery, motor symptoms (Movement Disorder Society Unified Parkinson's Disease Rating Scale III section, MDS-UPDRS-III) and complications (MDS-UPDRS-IV) severity, and LEDD before surgery. The percentage improvement in motor symptoms (M-OFF before vs. M-OFF/S-ON) and complications severity after DBS did not differ between groups, while LEDD reduction was greater in the STN- than GPi-DBS cohort (Table 1).

Table 1

Demographic and clinical characteristics of patients included in the analysis. Abbreviations: PD: Parkinson's disease; UPDRS: Movement Disorder Society-Unified Parkinson's Disease Rating Scale; LEDD: Levodopa Equivalent Daily Dose; STN: Subthalamic Nucleus; GPi: Globus Pallidus internus; IQR: interquartile range. Statistically significant values ($p < 0.05$) are highlighted in bold. [a] Percentage changes before and after surgery, computed as $[(Value_{PRE}-Value_{POST})/Value_{PRE})*100]$. [b] P-values refer to the results of between-target comparison (STN vs. GPi)

Subject	Target	Age	Sex	PD duration (y)*	UPDRS III MOFF pre	UPDRS III MOFF post	Change UPDRS-III(%)[a]	UPDRS IV pre	UPDRS IV post	Change UPDRS IV (%)[a]	LEDD pre-	LEDD post-	Change LEDD (%)[a]
1	STN	62	M	12	46	38	-17.4	8	7	-12.5	1290	595	-53.9
2	STN	65	M	14	48	41	-14.6	9	10	11.1	1507	839	-44.3
3	STN	51	M	14	36	34	-5.6	8	2	-75.0	661	505	-23.6
4	STN	70	F	12	45	35	-22.2	9	3	-66.7	1260	280	-77.8
5	STN	50	F	17	44	38	-13.6	15	7	-53.3	1186	300	-93.3
6	STN	53	F	6	26	29	11.5	12	3	-75.0	1305	400	-69.3
7	STN	58	M	13	56	45	-19.6	12	2	-83.3	1055	200	-81.0
8	STN	65	F	9	41	22	-46.3	15	8	-46.7	700	325	-53.6
9	STN	47	M	7	45	34	-24.4	10	6	-40.0	1502	550	-63.4
10	STN	61	M	12	45	23	-48.9	11	4	-63.6	1327	570	-57.0
11	STN	62	M	13	54	42	-22.2	9	4	-55.6	2100	850	-59.5
12	STN	68	F	7	57	42	-26.3	14	5	-64.3	945	320	-66.1
13	GPi	57	F	11	76	53	-30.3	10	4	-60.0	1550	720	-53.5
14	GPi	62	F	17	54	42	-22.2	13	6	-53.8	1185	835	-29.5
15	GPi	60	M	13	41	38	-7.3	10	8	-20.0	1243	855	-31.2
16	GPi	64	F	17	56	47	-16.1	16	4	-75.0	1325	500	-62.3
17	GPi	45	M	9	74	62	-16.2	15	10	-33.3	875	425	-51.4
18	GPi	71	F	9	38	28	-26.3	7	1	-85.7	690	450	-34.8
19	GPi	68	M	23	62	50	-19.4	11	7	-36.4	1113	955	-14.2
20	GPi	54	M	13	47	37	-21.3	14	4	-71.4	850	400	-52.9
21	GPi	43	M	16	29	12	-58.6	3	1	-66.7	580	220	-62.1
Median (IQR) STN	-	61.5 (12.5)		12 (4.7)	45 (6.2)	36.5 (8.5)	-20.1 (10.5)	10.5 (3.5)	4.5 (4)	-59.6 (23.7)	1275 (343.2)	452 (272.5)	-61.4 (17.6)
Median (IQR) GPi	-	60 (10)		13 (6)	54 (21)	42 (13)	-21.2 (10.1)	11 (4)	4 (3)	-60 (35)	1113 (393)	500 (410)	-51.4 (22.3)
P value[b]	-	0.8	1.0	0.19	0.1	0.2	0.7	0.9	0.7	0.8	0.3	0.2	**0.02**

When considering changes in cardinal motor symptoms in our specific experimental setting, L-Dopa administration (M-OFF/S-OFF vs. M-ON/S-OFF) similarly reduced MDS-UPDRS-III composite scores (bradykinesia+rigidity+tremor) in STN- ($p < 0.001$, mean change: -34.4%) and GPi-DBS ($p < 0.001$, mean change: -31.9%) cohorts (STN-DBS vs. GPi-DBS: $p = 0.2$). Importantly, there was no difference in L-Dopa doses administered between groups (STN median [IQR]: 100[0] mg; GPi:100[16.5] mg, $p = 0.12$). DBS (M-OFF/S-OFF vs. M-OFF/S-ON) also improved motor scores to a comparable extent between groups (STN-DBS: $p < 0.001$, mean change: -31.1%; GPi-DBS: $p < 0.001$, mean change: -29.2%, STN- vs. GPi-DBS: $p = 0.1$). As expected, the TEED of STN-DBS (median [IQR]: 192.8[138.5] μJ/s) was lower than GPi-DBS (median [IQR]: 435.4[274.9] μJ/s), with a significant between-group difference ($p < 0.0001$, Supplementary Table I)[4,7].

Beta activity and reactivity to L-Dopa and DBS in STN and GPi

In the M-OFF/S-OFF condition, no significant frequency-wise differences in beta power or burst characteristics were observed between STN and GPi (Fig. 2). However, when comparing these parameters computed around the individual beta peak, we found that beta peak amplitude was higher and burst duration longer in the STN than GPi (Fig. 2). Notably, peak frequency distribution was similar between targets ($p = 0.11$, Supplementary Fig. 1).

Effects of L-Dopa

L-Dopa (M-ON/S-OFF vs. M-OFF/S-OFF) modulated beta power in both targets, but a frequency specificity emerged in its effect (Fig. 3). Indeed, medication selectively reduced low-beta power in the STN (13–18 Hz), while suppressing higher beta frequencies in the GPi (20–23 Hz). This difference was also confirmed when directly comparing the two cohorts, where a significant cluster at 13–15 Hz was present between targets (Fig. 3 and Table 2). Frequency-specific effects of L-Dopa were also found in the bin-wise analysis of bursts, which showed reduced duration and increased rate in the low-beta range when considering the STN (13–18 Hz), and no change in the GPi. In line with the within-group results, between-target comparison showed a significant cluster at 14–16 Hz (Fig. 3, Supplementary Fig. 2, and Table 2). The analysis performed around the beta peak disclosed that L-Dopa reduced peak amplitude and burst duration, and increased burst rate in both nuclei, but the magnitude of peak amplitude reduction was greater in the STN than GPi (Fig. 3, Supplementary Fig. 3, and Table 2).

Table 2
Results of frequency-resolved and peak-centred cluster-based permutation test.

		STN		GPi		STN vs. GPi	
		cluster range	*p value*	*cluster range*	*p value*	*cluster range*	*p value*
Frequency-resolved analysis							
Medication	power	13–18 Hz	0.002	20–23 Hz	0.01	13–15 Hz	0.03
	burst duration	13–18 Hz	< 0.001	n.s.		14–16 Hz	0.02
	burst rate	13–18 Hz	< 0.001	n.s.		n.s.	
Add-on Medication	power	13–14 Hz	0.001	20–21 Hz	0.03	13–14 Hz	0.02
	burst duration	n.s.		n.s.		n.s.	
	burst rate	n.s.		n.s.		n.s.	
Stimulation	power	14–30 Hz	< 0.001	20–27 Hz	< 0.001	15–16 Hz	0.03
	burst duration	13–17 Hz 20–27 Hz	0.002 <0.001	20–22 Hz	0.01	n.s.	
	burst rate	15–27 Hz	< 0.001	20–22 Hz 26–27 Hz	0.01 0.03	n.s.	
Add-on Stimulation	power	20–30 Hz	0.001	18–30 Hz	0.02	n.s.	
	burst duration	20–23 Hz 27–29 Hz	0.007 0.01	19–20 Hz 23–27 Hz	0.03 0.002	n.s.	
	burst rate	20–23 Hz 27–29 Hz	0.005 0.01	19–20 Hz 23–27 Hz	0.04 0.001	n.s.	
Medication + Stimulation	power	13–30 Hz	< 0.001	16–29 Hz	< 0.001	n.s.	
	burst duration	13–17 Hz 19–29 Hz	0.003 <0.001	14–20 Hz 24–28 Hz	0.001 0.006	n.s.	
	burst rate	13–21 Hz 23–27 Hz	< 0.001 0.003	16–20 Hz 24–27 Hz	0.004 0.01	n.s.	
Peak-centered analysis							
Medication	power	-3 / 3 Hz	< 0.001	-2 / 2 Hz	< 0.001	-1 / 0 Hz	0.03
	burst duration	-1 / 0 Hz	0.01	-1 / 0 Hz	0.01	n.s.	
	burst rate	-1 / 1Hz	0.003	− 1 / 0 Hz	0.02	n.s.	
Add-on Medication	power	0 / 2 Hz	0.001	n.s.		n.s.	
	burst duration	n.s.		n.s.		n.s.	
	burst rate	n.s.		n.s.		n.s.	
Stimulation	power	-2 / 3 Hz	< 0.001	-2 / 2 Hz	0.002	-1 / 1 Hz	0.004
	burst duration	-1 / 1 Hz	0.002	-1 / 2 Hz	< 0.001	n.s.	
	burst rate	-1 / 3 Hz	< 0.001	0 / 2 Hz	0.003	n.s.	
Add-on Stimulation	power	-1 / 3 Hz	< 0.001	0 / 1 Hz	0.03	n.s.	
	burst duration	n.s.		n.s.		n.s.	
	burst rate	n.s.		n.s.		n.s.	
Medication+ Stimulation	power	-2 / 3 Hz	< 0.001	-2 / 3 Hz	< 0.001	-1 / 1 Hz	< 0.001
	burst duration	-1 / 2 Hz	< 0.001	-1 / 2 Hz	0.002	n.s.	
	burst rate	-1 /2 Hz	< 0.001	-3 / 2 Hz	< 0.001	n.s.	

Abbreviations: Medication: M-OFF/S-OFF vs. M-ON/S-OFF; Add-on medication: M-OFF/S-ON vs. M-ON/S-ON; Stimulation: M-OFF/S-OFF vs. M-OFF/S-ON. Add-on stimulation: M-ON/S-OFF vs. M-ON/S-ON; Medication+Stimulation: M-OFF/S-OFF vs. M-ON/S-ON. Abbreviations: STN: Subthalamic Nucleus; GPi: Globus Pallidus internus; n.s.: no significant clusters.

Effects of DBS

DBS (M-OFF/S-ON vs. M-OFF/S-OFF) induced a broadband beta power reduction in the STN (14–30 Hz), and selective suppression of high-beta power in the GPi (20–27 Hz), with significant between-target differences in the low-beta range (15–16 Hz, Fig. 4 and Table 2). Similarly, beta bursts duration shortening and burst rate increase involved a beta broadband in the STN (13–17 Hz and 20–27 Hz for both measures), while it impacted only the high-beta sub-band in the GPi (20–22 Hz, Fig. 4, Supplementary Fig. 2, and Table 2). When specifically considering the individual beta peaks, DBS suppressed peak amplitude, shortened beta bursts and increased burst rate in both targets, with a stronger effect in the STN for the former parameter (Fig. 4, Supplementary Fig. 3, and Table 2).

Combined effects of L-Dopa and DBS

Adding L-Dopa to DBS (M-ON/S-ON vs. M-OFF/S-ON) determined neurophysiological effects on beta power overlapping those produced by L-Dopa alone. That is, the medication selectively suppressed low-beta power in the STN (13–14 Hz) and higher frequencies in the GPi (20–21 Hz), with a significant difference in the low-beta range (13–14 Hz) between targets (Supplementary Fig. 4 and Table 2). Importantly, L-Dopa add-on to DBS further decreased beta peak amplitude in the STN, but that effect was not evident in the GPi cohort (Supplementary Fig. 4 and Table 2). No change in beta bursts characteristics was found in STN and GPi, both in frequency-wise and around-the-peak analyses (Supplementary Figs. 2, 3 and 4, Table 2).

Adding DBS to L-Dopa (M-ON/S-ON vs. M-ON/S-OFF) reduced beta power (STN: 20–30 Hz; GPi: 18–30 Hz), burst duration, and rate selectively in the high-beta range (STN: 20–23 Hz and 27–29 Hz for both measures; GPi: 19–20 Hz and 23–27 Hz for both measures), and to a comparable extent between STN and GPi (Supplementary Figs. 2 and 5, Table 2). The beta peak amplitude was also further suppressed by adding stimulation to the medication, without significant between-target differences, while burst duration and rate, computed around the individual peak, remained unchanged in both targets (Supplementary Figs. 3 and 5, Table 2).

The combination of L-Dopa and DBS (M-ON/S-ON vs. M-OFF/S-OFF) induced a decrease in broadband beta power in both the STN (13–30 Hz) and GPi (16–29 Hz), to a comparable extent between the targets (Fig. 5 and Table 2). Similarly, beta bursts modulation involved both the low- and high-beta sub-bands in both targets (Fig. 5, Supplementary Fig. 2 and Table 2). Individual peak amplitude and around-the-peak burst duration decreased in both STN and GPi. However, the degree of beta peak suppression was again higher in the STN (Fig. 5 and Table 2).

We found a direct relationship between beta peak amplitude in the M-OFF/S-OFF condition and the amount of beta peak amplitude suppression induced by L-Dopa, DBS, and their combination (medication: $R = -0.52$, $p = 0.03$; stimulation: $R = -0.72$, $p < 0.001$; medication+stimulation: $R = -0.74$, $p < 0.001$).

Figure 6 summarises the effects of L-Dopa and DBS (alone and combined) on beta power in the STN and GPi.

Clinical-neurophysiological correlations

In the M-OFF/S-OFF condition, the severity of bradykinesia+rigidity correlated positively with low-beta power in the STN (15 Hz: $R = 0.64$, $p = 0.001$; 16 Hz: $R = 0.52$, $p = 0.02$) and the power in a higher beta frequency range in the GPi (19 Hz: $R = 0.51$, $p = 0.03$). A similar frequency-specific relationship was also present with beta burst duration (STN, 12–15 Hz: $0.55 < R < 0.82$, $0.001 < p < 0.03$; GPi, 20 Hz, $R = 0.53$, $p = 0.03$) (Fig. 2).

Importantly, the relationship between clinical measures and beta power in different frequency ranges based on the cohort tested was consistent, even when considering changes induced by medication and stimulation. Indeed, both L-Dopa-, DBS- and combined L-Dopa + DBS-induced changes in bradykinesia+rigidity severity were related to the amount of reduction in low-beta power for the STN (medication effect, 15 Hz: $R = 0.51$, $p = 0.03$, and 16 Hz: $R = 0.58$, $p = 0.007$; stimulation effect, 16 Hz: $R = 0.57$, $p = 0.01$; medication+stimulation effect, 14 Hz: $R = 0.61$, $p = 0.01$) and in the power of higher beta frequencies for the GPi (medication effect, 20 Hz: $R = 0.54$, $p = 0.02$; stimulation effect, 20 Hz: $R = 0.51$, $p = 0.03$, and 21 Hz: $R = 0.63$, $p = 0.008$, medication+stimulation effect, 21 Hz: $R = 0.52$, $p = 0.03$) (Figs. 3, 4 and 5, Supplementary Table 3).

Finally, we did not find any other relationship between neurophysiological and other clinical measures, including tremor severity, or their changes following L-Dopa or DBS (see Supplementary Table 2). Furthermore, no significant correlation was observed between percentage changes of peak amplitude and burst duration and clinical improvement with medication or stimulation (see Supplementary Table 3).

Discussion

In this study, we compared beta activity in chronic LFPs recorded from the STN and GPi in PD patients and their modulation by L-Dopa and DBS. Although beta dynamics were generally similar in the untreated state, both therapies induced frequency-specific effects across targets, with beta modulation shifted towards higher frequencies in the GPi. Moreover, individual beta peak amplitude was lower and less responsive in the GPi. Clinical-neurophysiological correlations supported a more prominent pathophysiological role of high-beta oscillations in the GPi than in the STN.

Together, these findings indicate target-specific responsiveness to therapy between STN and GPi, highlighting functional specialization despite integration within the same cortico-basal-thalamo-cortical network.

In the untreated state (M-OFF/S-OFF condition), beta power and bursting characteristics were comparable between nuclei, consistent with previous intraoperative LFP studies[35,36]. This similarity might reflect the inclusion in common cortico-basal networks, and shared exposure to aberrant beta synchronisation pathologically emerging within these circuits in PD[23,36]. However, beta peak amplitude was more prominent in the STN compared to the GPi, possibly reflecting intrinsically more tuned local subthalamic beta synchronisation.

Differences in spectral dynamics between targets became evident when assessing the differential responsiveness to medication and stimulation. To date, L-Dopa-induced changes in pallidal beta activity have been poorly characterised, and a comprehensive comparison with STN neurophysiological dynamics is lacking. Our findings demonstrated that L-Dopa effects on beta dynamics differ in frequency specificity and magnitude between targets. In the STN, beta power suppression and burst modulation (i.e., reduced duration and increased rate) selectively involved low-beta oscillations, in line with previous studies[17,18,20,25,26], while in the GPi L-Dopa effects on beta power were shifted towards the higher beta frequency range. Notably, this distinct frequency-specific modulation persisted during stimulation. These results expand previous findings reporting a general L-Dopa-induced reduction of beta mean power in the GPi[37,42], and greater high-beta power in the STN than GPi in the medication ON state[23]. The presence of dopaminergic modulation towards higher beta frequencies in the GPi might stem from the differential anatomical connections compared to STN and the pallidal role as the main output nucleus of the basal ganglia[11,43,44]. Because the GPi is positioned downstream of striatal dopaminergic modulation, its activity likely reflects an integrated output of multiple basal ganglia pathways, and restoring striatal dopaminergic tone might shape GPi beta activity more indirectly compared to the STN. In turn, this might produce effects that more closely resemble those observed in the sensorimotor cortex, where dopaminergic medication selectively modulates high-beta activity, in line with the GPi role as an output structure[22,45,46].

Furthermore, medication exerted more focused effects on pallidal burst dynamics compared to the STN. Despite comparable L-Dopa doses administered between cohorts, modulatory effects were observed only for bursts computed at the beta peak frequency, whereas frequency-resolved analysis did not reveal changes in burst characteristics. Again, this pattern might reflect a more indirect downstream dopaminergic influence on the GPi, affecting beta temporal dynamics (i.e., beta bursts) by specifically modulating spectral peaks rather than producing broader band-wide effects[41].

In our study, we also compared changes in beta power and bursts in response to DBS between targets. In line with previous research[17,27,47,48], we observed a broadband beta suppression and burst shortening in the STN. Conversely, the spectral and bursting modulation selectively involved higher beta frequencies in the GPi, with a significant between-target difference in the low-beta range. Given the distinct anatomical connectivity of the two targets, we speculate that DBS might exert its effects by differently modulating local pathological oscillations more functionally linked to abnormal high-beta activity across cortico-basal networks. GPi-DBS might more directly block high beta signals from propagating to the thalamus and be transmitted to the cortex, while STN-DBS could act more directly (antidromically) on cortical inputs. The similar final effects described on the motor cortex of STN and GPi-DBS and similar clinical benefits might be sustained by modulation of different but overlapping pathways, i.e., the hyperdirect pathway in the STN and motor thalamus in the GPi[4,7,22,23,49,50]. Overall, this finding further supports functional dissociation of beta sub-bands across the motor network.

The similar effect of L-Dopa and DBS on frequency-specific beta dynamics in the GPi deserves a comment, as it underscores that both interventions may target convergent nodes within the broader cortico-basal-thalamic loop. This convergence indicates that modulation of higher beta synchronisation in the GPi might represent a final common pathway through which both dopaminergic therapy and electrical stimulation restore more physiological motor network dynamics, especially long-range communications in the high-beta range[22,23,49]. In this regard, it was recently hypothesised that L-Dopa and DBS might have differential effects and mechanisms of action in the STN[22]. We here speculate that these mechanisms might display a higher overlap in the GPi, potentially mediated by the converging influence from other structures, reflecting the functional role of the nucleus as the main basal ganglia output structure.

Importantly, the different patterns in L-Dopa and DBS-induced modulation of beta dynamics between targets have also pathophysiologically relevant implications. Clinical-neurophysiological correlation analyses disclosed that lateralized bradykinesia+rigidity severity in the untreated state, as well as its changes after L-Dopa and DBS, were related to low-beta activity in the STN[25,38,51], while the relationship was shifted towards higher beta frequencies in the GPi. These data indicate that exaggerated oscillations in different beta sub-bands between STN and GPi have a role in the pathophysiology of cardinal motor symptoms in PD[17,25,51].

Another novel finding of our study concerns the combined effect of medication and stimulation, which showed a similar broadband modulation of beta power and bursts between targets. This might indicate that although medication and stimulation might differently affect STN and GPi activity, their combination converges into a common suppression of pathological beta activity across the cortico-basal networks. Specifically, in the GPi, low-beta suppression emerges only when both DBS and L-Dopa are simultaneously active, whereas in the STN, DBS alone is sufficient to attenuate both low- and high-beta components. This differential sensitivity could reflect distinct mechanisms of pathophysiological modulation within the two

nuclei and might provide a neurophysiological link for the clinical observation that L-Dopa doses are usually maintained after GPi-DBS, whereas they can be substantially reduced following STN-DBS[4,7,52].

Finally, when specifically assessing possible differences in L-Dopa and DBS effects on individual beta peaks between targets, we found that medication, stimulation, and their combination significantly reduced beta peaks in both targets. These data suggest that, despite frequency-specific effects, the treatments might act by reducing the dominant pathological beta synchronisation in both STN and GPi. However, L-Dopa and DBS suppressed the beta peak more strongly in the STN than GPi, which may reflect a prominent downregulation of excessive beta oscillations in the former target.

Besides adding pathophysiological insights to the role of GPi in PD, the results of our study have translational relevance for the development of tailored aDBS strategies. While supporting the use of beta activity as a robust physiomarker for pallidal aDBS, our findings suggest that higher beta frequencies could be more appropriate for guiding stimulation in the GPi in PD compared to STN[35,36,53]. Although aDBS has been recently approved for PD, beta reactivity to medication under chronic GPi-DBS has never been assessed, and GPi-aDBS stimulation programming is based on findings from research on STN-DBS. Our results offer the theoretical basis to guide aDBS with target-specific beta frequencies. The difference we observed in beta peak prominence and reactivity between STN and GPi also has clinical relevance. The use of the beta peak as a feedback signal is indeed a crucial step for aDBS programming[33,54]. Since beta peak amplitude appeared less sensitive to L-Dopa add-on to DBS in the GPi than STN, it might be more appropriate to use narrower LFP thresholds when programming GPi-aDBS.

Our study has some limitations. First, the sample size was relatively small, and larger future studies are needed to confirm the generalisability of our findings. Furthermore, L-Dopa effect was assessed after > 6 hours of withdrawal (clinical OFF condition), potentially resulting in incomplete wash-out. However, due to the severity of motor symptoms and OFF-state troublesome phenomena, some patients would not have tolerated longer withdrawal periods. Similarly, the effects of stimulation were assessed 5 minutes after DBS was turned off. Although an incomplete DBS wash-out cannot be entirely excluded, this interval is likely sufficient, as previously demonstrated[48].

Concluding, our findings demonstrate that STN and GPi display target-specific changes in beta dynamics in response to L-Dopa and DBS in PD. L-Dopa selectively reduced low-beta oscillations and DBS modulated beta activity broadly in the STN, whereas both interventions predominantly modulated high-beta activity in the GPi. This frequency-specificity likely reflects the downstream integrative role of GPi within basal ganglia circuits. The similar high-beta modulation induced by L-Dopa and DBS in the GPi suggests partly convergent mechanisms, whereby dopaminergic and electrical therapies might restore physiological network activity through distinct but overlapping pallido-thalamo-cortical pathways. Overall, these results emphasise functional dissociation within the pathological beta spectrum across the basal ganglia nodes and support the use of frequency-tailored neuromodulation strategies based on target-specific beta dynamics, with higher beta frequencies being a more informative biomarker for aDBS in GPi compared to STN.

Materials and Methods

Participants

Twenty-one patients with advanced PD treated with bilateral STN- (12 patients, 5 females, 24 hemispheres) or GPi-DBS (9 patients, 4 females, 18 hemispheres) were included. Clinical and demographic characteristics of patients are summarised in Table 1. All patients were implanted with the sensing-enabled Medtronic Percept™ PC neurostimulator and SenSight™ directional leads (B33005). All subjects gave their written informed consent to participate in the study, research was approved by the Local Ethics Committee of Padua Province, and completed in accordance with the Declaration of Helsinki.

Experimental protocol and data acquisition

Assessments were performed in a chronic stimulation setting, > 6 months after surgery and at least 1 month after stable stimulation parameters. Each subject was evaluated in a single session in the clinical OFF condition (> 6 hours after the last L-Dopa intake, M-OFF) and 1 hour after the administration of the usual L-Dopa dose (M-ON, Supplementary Table 1). In each medication condition, patients were assessed before and ≈ 5 minutes after switching off DBS (S-ON and S-OFF, respectively), resulting in four different conditions and clinical states: i) M-OFF/S-ON; ii) M-OFF/S-OFF; iii) M-ON/S-ON and iv) M-ON/S-OFF (Fig. 1). Clinical and neurophysiological data were collected in each condition. Appendicular motor signs were evaluated using the rigidity (3.3), bradykinesia (3.4–3.8), and tremor (3.15–3.18) subitems of the third section of the MDS-UPDRS-III. Neurophysiological data were acquired with patients comfortably seated in an armchair and instructed to rest while keeping their eyes open. LFPs were recorded using the BrainSense™ Streaming feature from the contact pair adjacent to the patient's chronic stimulating level with a sampling rate of 250 Hz. Stimulation parameters (amplitude, pulse width and frequency) used for chronic DBS were used in S-ON conditions (Supplementary Table 1). Data were exported as .json files for further offline analyses.

Data analysis

All data were analysed offline in MATLAB R2022b (The MathWorks Inc., Natick, Massachusetts). LFPs were extracted with the open-source Perceive toolbox (https://github.com/neuromodulation/perceive/). For each subject, 120 s of motion artefact-free signals were selected for each condition

for subsequent analyses. A 5th-order Butterworth filter was applied at 5 Hz high-pass and 98 Hz low-pass to minimise movement- and stimulation-related artefacts. Filtered signals were then visually inspected for electrocardiogram (ECG) or stimulation contamination. When ECG artefacts were detected, signals were further processed using a customised Template Subtraction Method, in which R-peaks from the QRS complex were identified and then subtracted from the original LFP signal[55].

Power spectral density was estimated using Welch's method with 1-s windows and 50% overlap. Spectra were normalised to the total power as a sum across the frequency range 5–45 Hz and expressed as a percentage of the total sum[22,48,51]. Beta peaks within the 13–30 Hz range were identified using the *findpeaks* MATLAB function, then visually inspected, reviewed, and modified if needed(see Supplementary Fig. 1 for beta peak distributions)[17].

Beta bursts were computed for each frequency bin (1 Hz) across the entire beta range (13–30 Hz) by applying a bandpass filter (± 2 Hz) around each frequency bin, allowing for a frequency-resolved characterisation of bursting activity[20]. To detect bursts, the Hilbert envelope of the filtered signal was computed, and bursts were defined as segments where amplitude exceeded the 75th percentile threshold, separately for each condition[26]. To control for frequency-dependent effects, a minimum burst length of 2/frequency (s) was applied[21,24]. For each condition, burst duration (time between consecutive threshold crossings) and rate (number of bursts/second) were calculated.[26] In a separate additional analysis, bursts were computed within the ± 3 Hz range around the individual beta peak frequency in the M-OFF/S-OFF condition using the same approach.

Statistical analysis

The Fisher's exact test and Mann-Whitney U test were used to analyse possible differences in clinical and demographic characteristics between STN- and GPi-DBS cohorts.

Separate cluster-based permutation tests were performed to assess differences in spectral power and burst characteristics (duration and rate) across the beta range (13–30 Hz) and around the beta peak (± 3 Hz): i) between different conditions in STN and GPi (paired tests), and ii) between targets (unpaired tests). In all cases, differences were randomly permuted 10000 times for a subset of hemispheres. For each frequency point, the z-statistic of the actual mean gradient/gradient difference was computed based on the distribution of the 10000 permutations. The supra-threshold clusters (pre-cluster threshold: $p < 0.05$) were determined for each permutation, and the sum of the z-statistics within these clusters was stored to form a distribution[56]. A two-sample Kolmogorov-Smirnov test was used to compare the distribution of beta peak frequency between targets.

Spearman's correlation was performed to assess clinical-neurophysiological relationships. To this purpose, spectral characteristics and burst parameters were correlated with the MDS-UPDRS-III lateralized composite bradykinesia+rigidity, and tremor subscores. To assess possible correlations between modifications in neurophysiological and clinical variables, percentage changes in PSD and MDS-UPDRS-III subscore were computed as $[((ON_{value}\text{-}OFF_{value})/OFF_{values})*100]$. To control for multiple comparisons, p-values were corrected for false discovery rate (FDR) using the Benjamini-Hochberg procedure.

Clinical and demographic characteristics are reported as median and interquartile range (IQR). Statistical analyses were performed using MATLAB R2022b. A $p < 0.05$ was considered significant in all statistical analyses.

Declarations

Contributions

Conception of the work and project design: V.D., A.G. and A.A. Data collection: V.D., D.C., L.L.G. and S.P. Data analysis: V.D., A.Av., E.B. and C.P. Interpretation of data, manuscript draft, revision and editing: V.D., G.T., A.Av., A.L., C.P., A.A. and A.G. All authors read and approved the final submission.

Corresponding author

Correspondence to Andrea Guerra.

Ethics declarations

Competing Interests

The authors declare the following competing interests: G.T. received financial support from Boston Scientific and Medtronic, not related to the present work. G.T., A.Av. and E.B. receive funding from the Swiss National Science Foundation (project number: PZ00P3_202166), not related to the present work. G.T. and A.Av. received funding from the Swiss Parkinson Association. A.A. has received honoraria/consultation fees from AbbVie, Bial, Bayer, Stada, Covantec, Ever Pharma, Medscape, Roche, Theravance Biopharma, UCB, and Zambon, , not related to the present work. A.A. has also received funding from Horizon 2020 - Ministry of University and Research (MIR), Ministry of Health (MOH), European Union - NextGenerationEU

– NRRP M6C2 - Investment: 2.1 "Enhancement and strengthening of biomedical research within the NSH", not related to the present work. A.G. has received compensation for consultancy and speaker-related activities from Bial, Zambon, STADA; he receives funding from the European Union “Next Generation EU, Mission 4 Component 1, Project code: P20223HHZ8, CUP: C53D23008440001”, not related to the present work.

Author Contribution

Conception of the work and project design: V.D., A.G. and A.A. Data collection: V.D., D.C., L.L.G. and S.P. Data analysis: V.D., A.Av., E.B. and C.P. Interpretation of data, manuscript draft, revision and editing: V.D., G.T., A.Av., A.L., C.P., A.A. and A.G. All authors read and approved the final submission.

Acknowledgments

This work received no funding.

Data Availability

The data obtained in this research are available from the corresponding author upon reasonable request.

References

1. Antonini, A., Moro, E., Godeiro, C. & Reichmann, H. Medical and surgical management of advanced Parkinson’s disease. *Mov. Disord.* **33**, 900–908 (2018).
2. Deuschl, G. *et al.* European Academy of Neurology/Movement Disorder Society-European Section Guideline on the Treatment of Parkinson’s Disease: I. Invasive Therapies. *Mov. Disord.* **37**, 1360–1374 (2022).
3. Lozano, A. M. *et al.* Deep brain stimulation: current challenges and future directions. *Nat. Rev. Neurol.* **15**, 148–160 (2019).
4. Follett, K. A. *et al.* Pallidal versus Subthalamic Deep-Brain Stimulation for Parkinson’s Disease. *NEJM* **362**, 2077–2091 (2010).
5. Mainardi, M. *et al.* Deep brain stimulation of globus pallidus internus and subthalamic nucleus in Parkinson’s disease: a multicenter, retrospective study of efficacy and safety. *Neurol. Sci.* **45**, 177–185 (2024).
6. Mei, S. *et al.* Three-Year Gait and Axial Outcomes of Bilateral STN and GPi Parkinson’s Disease Deep Brain Stimulation. *Front. Hum. Neurosci.* **14**, 1 (2020).
7. Odekerken, V. J. J. *et al.* Subthalamic nucleus versus globus pallidus bilateral deep brain stimulation for advanced Parkinson’s disease (NSTAPS study): a randomised controlled trial. *Lancet Neurol.* **12**, 37–44 (2013).
8. Wagle Shukla, A., Bange, M. & Muthuraman, M. Patient, target, device, and program selection for DBS in Parkinson’s disease: advancing toward precision care. *npj Parkinsons Dis.* **11**, 195 (2025).
9. Bolam, J. P., Hanley, J. J., Booth, P. A. C. & Bevan, M. D. Synaptic organisation of the basal ganglia. *J. Anat.* **196**, 527–542 (2000).
10. Emmi, A., Antonini, A., Macchi, V., Porzionato, A. & De Caro, R. Anatomy and Connectivity of the Subthalamic Nucleus in Humans and Non-human Primates. *Front. Neuroanat.* **14**, 13 (2020).
11. Obeso, J. A. & Lanciego, J. L. Past, Present, and Future of the Pathophysiological Model of the Basal Ganglia. *Front. Neuroanat.* **5**, 39 (2011).
12. Asadi, A., Madadi Asl, M., Vahabie, A.-H. & Valizadeh, A. The Origin of Abnormal Beta Oscillations in the Parkinsonian Corticobasal Ganglia Circuits. *Parkinsons Dis.* **2022**, 7524066 (2022).
13. Brown, P. *et al.* Dopamine Dependency of Oscillations between Subthalamic Nucleus and Pallidum in Parkinson’s Disease. *J. Neurosci.* **21**, 1033–1038 (2001).
14. Neumann, W.-J., Horn, A. & Kühn, A. A. Insights and opportunities for deep brain stimulation as a brain circuit intervention. *Trends Neurosci.* **46**, 472–487 (2023).
15. van Wijk, B. C. M., de Bie, R. M. A. & Beudel, M. A systematic review of local field potential physiomarkers in Parkinson’s disease: from clinical correlations to adaptive deep brain stimulation algorithms. *J Neurol.* **270**, 1162–1177 (2023).
16. Kühn, A. A. *et al.* Pathological synchronisation in the subthalamic nucleus of patients with Parkinson’s disease relates to both bradykinesia and rigidity. *Exp. Neurol.* **215**, 380–387 (2009).
17. Mathiopoulou, V. *et al.* Modulation of subthalamic beta oscillations by movement, dopamine, and deep brain stimulation in Parkinson’s disease. *npj Parkinsons Dis.* **10**, 77 (2024).
18. Priori, A. *et al.* Rhythm-specific pharmacological modulation of subthalamic activity in Parkinson’s disease. *Exp. Neurol.* **189**, 369–379 (2004).
19. Ray, N. J. *et al.* Local field potential beta activity in the subthalamic nucleus of patients with Parkinson’s disease is associated with improvements in bradykinesia after dopamine and deep brain stimulation. *Exp. Neurol.* **213**, 108–113 (2008).

20. Torrecillos, F., He, S., Kühn, A. A. & Tan, H. Average power and burst analysis revealed complementary information on drug-related changes of motor performance in Parkinson's disease. *npj Parkinsons Dis.* **9**, 1–13 (2023).
21. Alva, L. *et al.* Clinical neurophysiological interrogation of motor slowing: A critical step towards tuning adaptive deep brain stimulation. *Clin. Neurophysiol.* **152**, 43–56 (2023).
22. Binns, T. S. *et al.* Shared pathway-specific network mechanisms of dopamine and deep brain stimulation for the treatment of Parkinson's disease. *Nat. Commun.* **16**, 3587 (2025).
23. Oswal, A. *et al.* Neural signatures of hyperdirect pathway activity in Parkinson's disease. *Nat. Commun.* **12**, 5185 (2021).
24. Tinkhauser, G. *et al.* Beta burst coupling across the motor circuit in Parkinson's disease. *Neurobiol. Dis.* **117**, 217–225 (2018).
25. Lofredi, R. *et al.* Subthalamic beta bursts correlate with dopamine-dependent motor symptoms in 106 Parkinson's patients. *npj Parkinsons Dis.* **9**, 1–9 (2023).
26. Tinkhauser, G. *et al.* Beta burst dynamics in Parkinson's disease OFF and ON dopaminergic medication. *Brain* **140**, 2968–2981 (2017).
27. Anderson, R. *et al.* A Novel Method for Calculating Beta Band Burst Durations in Parkinson's Disease Using a Physiological Baseline. *J. Neurosci. Methods* **343**, 108811 (2020).
28. Anidi, C. *et al.* Neuromodulation targets pathological not physiological beta bursts during gait in Parkinson's disease. *Neurobiol. Dis.* **120**, 107–117 (2018).
29. Bange, M. *et al.* Subthalamic stimulation modulates context-dependent effects of beta bursts during fine motor control. *Nat. Commun.* **15**, 3166 (2024).
30. Tinkhauser, G. *et al.* The modulatory effect of adaptive deep brain stimulation on beta bursts in Parkinson's disease. *Brain* **140**, 1053–1067 (2017).
31. Averna, A. *et al.* Spectral Topography of the Subthalamic Nucleus to Inform Next-Generation Deep Brain Stimulation. *Mov. Disord.* **38**, 818–830 (2023).
32. D'Onofrio, V. *et al.* Local field potentials survey to guide DBS programming in Parkinson's disease: a clinical-neurophysiological longitudinal study. *npj Parkinsons Dis.* **12**, 1 (2025).
33. Neumann, W.-J., Gilron, R., Little, S. & Tinkhauser, G. Adaptive Deep Brain Stimulation: From Experimental Evidence Toward Practical Implementation. *Mov. Disord.* **38**, 937–948 (2023).
34. Shah, A. *et al.* Combining Multimodal Biomarkers to Guide Deep Brain Stimulation Programming in Parkinson Disease. *Neuromodulation* **26**, 320–332 (2023).
35. Eisinger, R. S. *et al.* Parkinsonian Beta Dynamics during Rest and Movement in the Dorsal Pallidum and Subthalamic Nucleus. *J. Neurosci.* **40**, 2859–2867 (2020).
36. Piña-Fuentes, D. *et al.* The characteristics of pallidal low-frequency and beta bursts could help implementing adaptive brain stimulation in the parkinsonian and dystonic internal globus pallidus. *Neurobiol. Dis.* **121**, 47–57 (2019).
37. Silberstein, P. Patterning of globus pallidus local field potentials differs between Parkinson's disease and dystonia. *Brain* **126**, 2597–2608 (2003).
38. Sumarac, S. *et al.* Clinico-physiological correlates of Parkinson's disease from multi-resolution basal ganglia recordings. *npj Parkinsons Dis.* **10**, 1–11 (2024).
39. Wang, D. D. *et al.* Pallidal Deep-Brain Stimulation Disrupts Pallidal Beta Oscillations and Coherence with Primary Motor Cortex in Parkinson's Disease. *J. Neurosci.* **38**, 4556–4568 (2018).
40. Jimenez-Shahed, J., Telkes, I., Viswanathan, A. & Ince, N. F. GPi Oscillatory Activity Differentiates Tics from the Resting State, Voluntary Movements, and the Unmedicated Parkinsonian State. *Front. Neurosci.* **10**, (2016).
41. Lofredi, R. *et al.* Pallidal beta bursts in Parkinson's disease and dystonia. *Mov. Disord.* **34**, 420–424 (2019).
42. Yin, Z. *et al.* Pathological pallidal beta activity in Parkinson's disease is sustained during sleep and associated with sleep disturbance. *Nat. Commun.* **14**, 5434 (2023).
43. Wichmann, T. Functional Aspects of the Basal Ganglia. in *Oxford Textbook of Movement Disorders* (ed. Burn, D.) (Oxford University Press, 2013).
44. Wichmann, T. & DeLong, M. R. Deep Brain Stimulation for Movement Disorders of Basal Ganglia Origin: Restoring Function or Functionality? *Neurotherapeutics* **13**, 264–283 (2016).
45. Smith, Y. & Villalba, R. Striatal and extrastriatal dopamine in the basal ganglia: An overview of its anatomical organization in normal and Parkinsonian brains. *Mov. Disord.* **23**, S534–S547 (2008).
46. Wei, K. *et al.* The effect of L-dopa and DBS on cortical oscillations in Parkinson's disease analyzed by hidden Markov model algorithm. *NeuroImage* **305**, 120992 (2025).
47. Eusebio, A. *et al.* Deep brain stimulation can suppress pathological synchronisation in parkinsonian patients. *J. Neurol. Neurosurg. Psychiatry* **82**, 569–573 (2011).

48. Feldmann, L. K. *et al.* Toward therapeutic electrophysiology: beta-band suppression as a biomarker in chronic local field potential recordings. *npj Parkinsons Dis.* **8**, 44 (2022).
49. Malekmohammadi, M., AuYong, N., Ricks-Oddie, J., Bordelon, Y. & Pouratian, N. Pallidal deep brain stimulation modulates excessive cortical high β phase amplitude coupling in Parkinson disease. *Brain Stimul.* **11**, 607–617 (2018).
50. Oswal, A. *et al.* Deep brain stimulation modulates synchrony within spatially and spectrally distinct resting state networks in Parkinson's disease. *Brain* **139**, 1482–1496 (2016).
51. Neumann, W.-J. *et al.* Subthalamic synchronized oscillatory activity correlates with motor impairment in patients with Parkinson's disease. *Mov. Disord.* **31**, 1748–1751 (2016).
52. Lachenmayer, M. L. *et al.* Subthalamic and pallidal deep brain stimulation for Parkinson's disease—meta-analysis of outcomes. *npj Parkinsons Dis.* **7**, 77 (2021).
53. Darcy, N. *et al.* Spectral and spatial distribution of subthalamic beta peak activity in Parkinson's disease patients. *Exp. Neurol.* **356**, 114150 (2022).
54. di Biase, L. *et al.* Adaptive, personalized closed-loop therapy for Parkinson's disease: biochemical, neurophysiological, and wearable sensing systems. *Expert Rev. Neurother.* **21**, 1371–1388 (2021).
55. Stam, M. J. *et al.* A comparison of methods to suppress electrocardiographic artifacts in local field potential recordings. *Clin. Neurophysiol.* **146**, 147–161 (2023).
56. Bernasconi, E. *et al.* Neurophysiological gradient in the Parkinsonian subthalamic nucleus as a marker for motor symptoms and apathy. *npj Parkinsons Dis* **11**, 4 (2025).

Figures

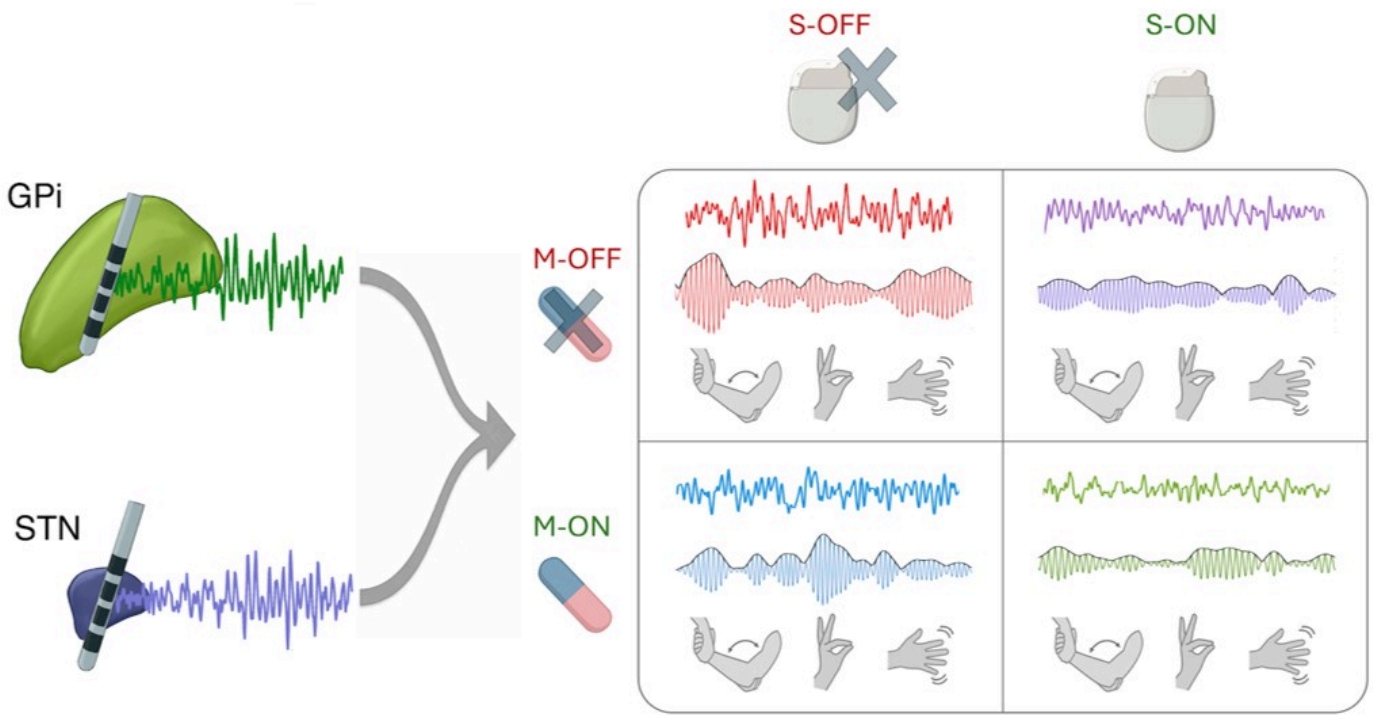


Figure 1

Signal acquisition protocol. Local Field Potentials (LFP) were recorded from Deep Brain Stimulation (DBS) electrodes implanted in Subthalamic Nucleus (STN) or Globus Pallidus internus (GPi) in four different conditions with respect to medication (L-Dopa) and stimulation: M-OFF/S-OFF (red exemplary raw signal and beta peak-filtered signal), M-OFF/S-ON (purple signals), M-ON/S-OFF (blue signals) and M-ON/S-ON (green signals). In each condition, clinical assessment of lateralized cardinal motor symptoms was performed after LFP recordings. Abbreviations: STN: Subthalamic Nucleus; GPi: Globus Pallidus internus; M-OFF: Medication OFF; M-ON: Medication ON; S-OFF: Stimulation OFF; S-ON: Stimulation ON.

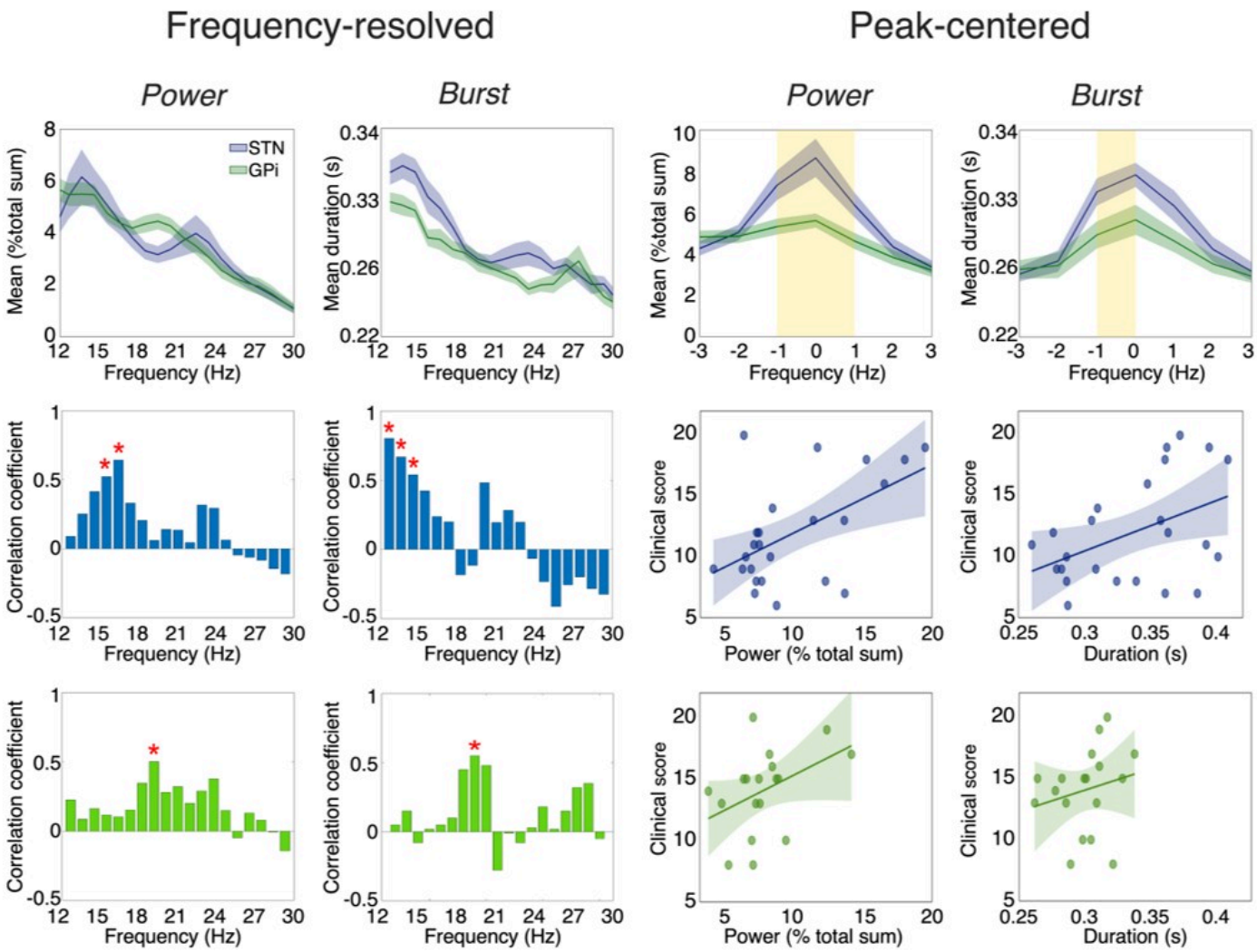


Figure 2

Baseline differences in beta power and burst durations between targets. Frequency-resolved and peak-centred (±3 Hz around individual beta peak) beta **power**and **burst duration**at baseline (M-OFF/S-OFF) are shown for the Subthalamic Nucleus (STN) and Globus Pallidus internus (GPi). Power spectra and burst durations are reported as means across subjects, shaded lines represent standard error, while yellow shaded bars indicate significant between-target differences ($p < 0.05$). Histograms display Spearman's correlation coefficients between beta metrics and bradykinesia+rigidity subscores; asterisks denote significant correlations ($p < 0.05$). Scatter plots show individual relationships between bradykinesia+rigidity subscores and peak-centred beta metrics. Abbreviations: STN: Subthalamic Nucleus; GPi: Globus Pallidus internus.

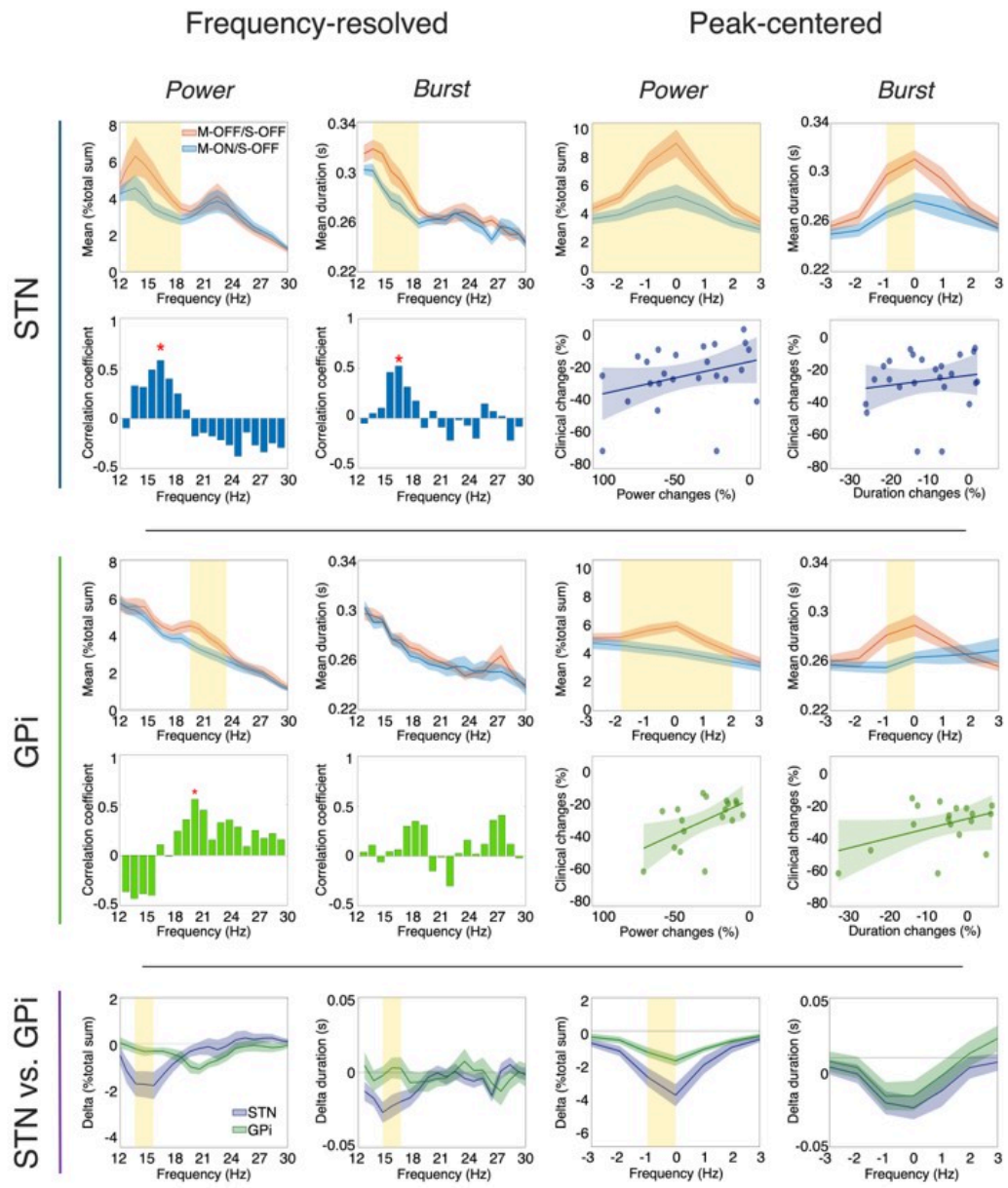


Figure 3

L-Dopa-induced modulation of beta power and burst duration in the STN and GPi and clinical correlations. Frequency-resolved (left) and peak-centred (±3 Hz around individual beta peak, right) beta **power** and **burst duration** are shown for the **STN (top)** and **GPi (middle).** Lines represent group means±SEM for M-OFF/S-OFF (red) and M-ON/S-OFF (blue) conditions. **Yellow shaded bars** indicate frequency ranges with significant L-Dopa effects (cluster-based permutation, $p < 0.05$). Histograms plot Spearman's correlation coefficients between percentage changes in beta metrics and changes in bradykinesia+rigidity subscores; asterisks denote significant correlations ($p < 0.05$). Scatter plots show individual relationships between percentage changes in bradykinesia+rigidity subscores and peak-centred beta metrics. The bottom row displays L-Dopa-induced changes (delta) in beta measures between STN (blue) and GPi (green). Abbreviations: STN: Subthalamic Nucleus; GPi: Globus Pallidus internus. M-OFF/S-OFF: Medication OFF/Stimulation OFF condition; M-ON/S-OFF: Medication ON/Stimulation OFF condition.

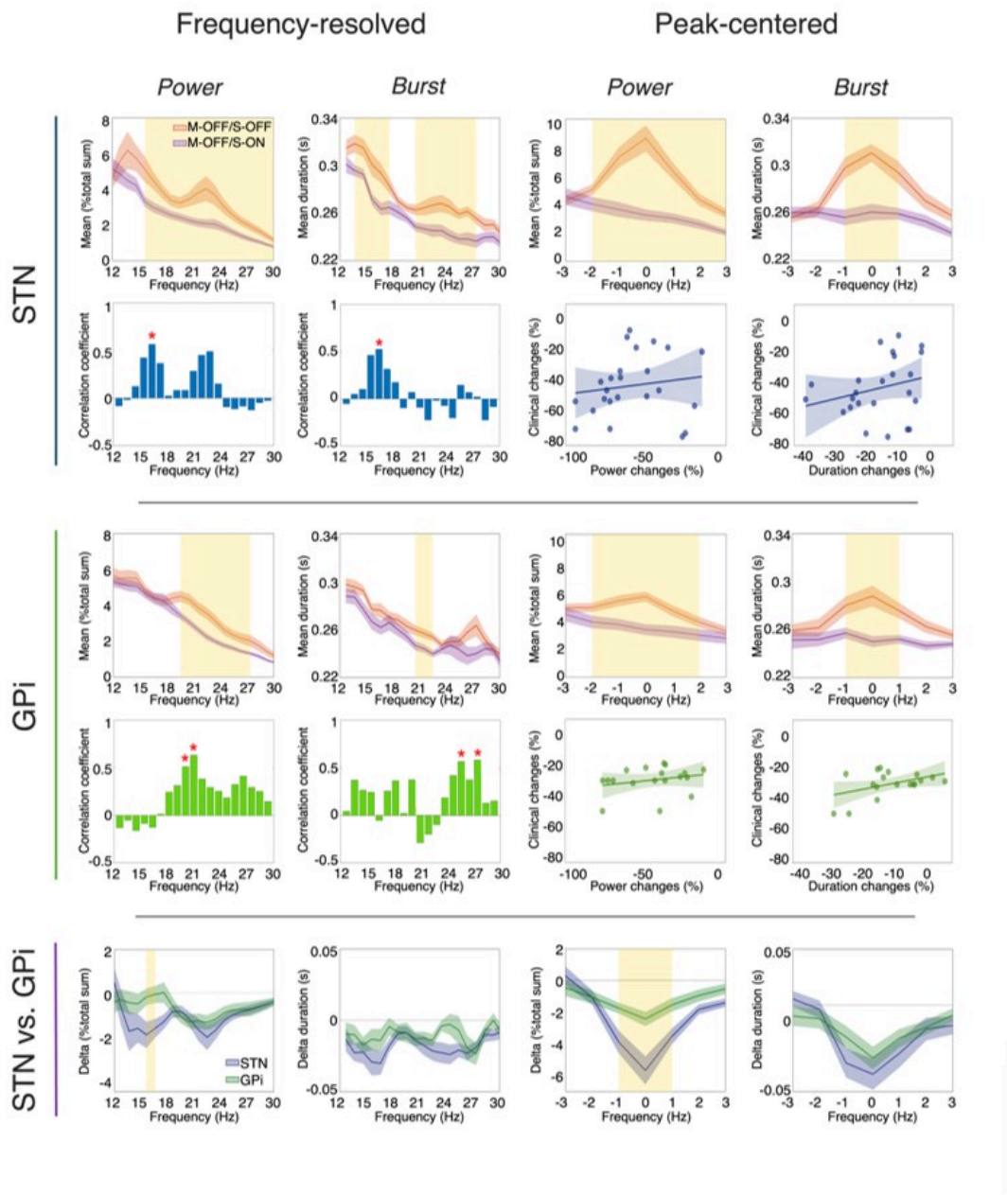


Figure 4

Stimulation-induced modulation of beta power and burst duration and clinical correlations in the STN and GPi. Cluster-based, frequency-resolved (left) and peak-centred (right) modulation of beta power and bursts durations between M-OFF/S-OFF and M-OFF/S-ON conditions in the STN (top) and GPi (middle). Lines represent group means, shaded bars standard error, while y**ellow shaded bars** indicate frequency ranges with significant stimulation-induced effects ($p < 0.05$). Histograms plot Spearman's correlation coefficients between percentage changes in beta metrics and changes in bradykinesia+rigidity subscores; asterisks denote significant correlations ($p < 0.05$). Scatter plots show individual relationships between bradykinesia+rigidity subscores and peak-centred beta changes. The bottom row compares delta changes in beta measures between STN (blue) and GPi (green). Abbreviations: STN: Subthalamic Nucleus; GPi: Globus Pallidus internus. Medication OFF/Stimulation OFF condition; M-OFF/S-ON: Medication OFF/Stimulation ON condition

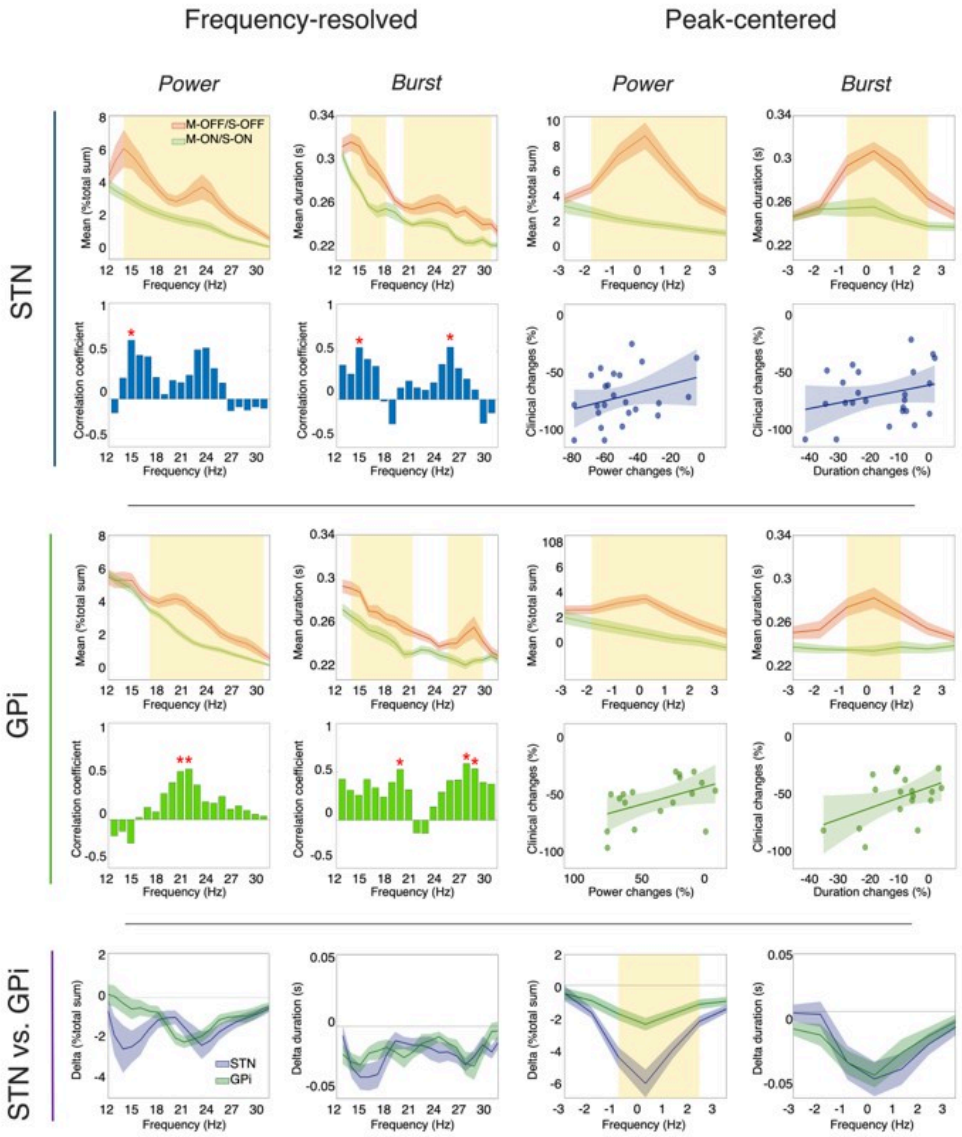


Figure 5

Combined L-Dopa and stimulation modulation of beta power and burst duration in STN and GPi and clinical correlations. Frequency-resolved (12–30 Hz, left) and peak-centred (±3 Hz around individual beta peak, right) beta **power** and **burst duration** are shown for the **STN (top)** and **GPi (middle).** Lines represent group means ± standard error for M-OFF/S-OFF (red) and M-ON/S-ON (green) conditions. **Yellow shaded bars** indicate significant results of the cluster-based permutation test. Histograms display Spearman's correlation coefficients between percentage changes in beta metrics and changes in bradykinesia+rigidity subscores; asterisks denote significant correlations ($p < 0.05$). Scatter plots show individual relationships between bradykinesia+rigidity subscores and peak-centred beta changes. The bottom row compares delta changes in beta measures between STN (blue) and GPi (green). Abbreviations: STN: Subthalamic Nucleus; GPi: Globus Pallidus internus. Medication OFF/Stimulation OFF condition; M-ON/S-ON: Medication ON/Stimulation ON condition

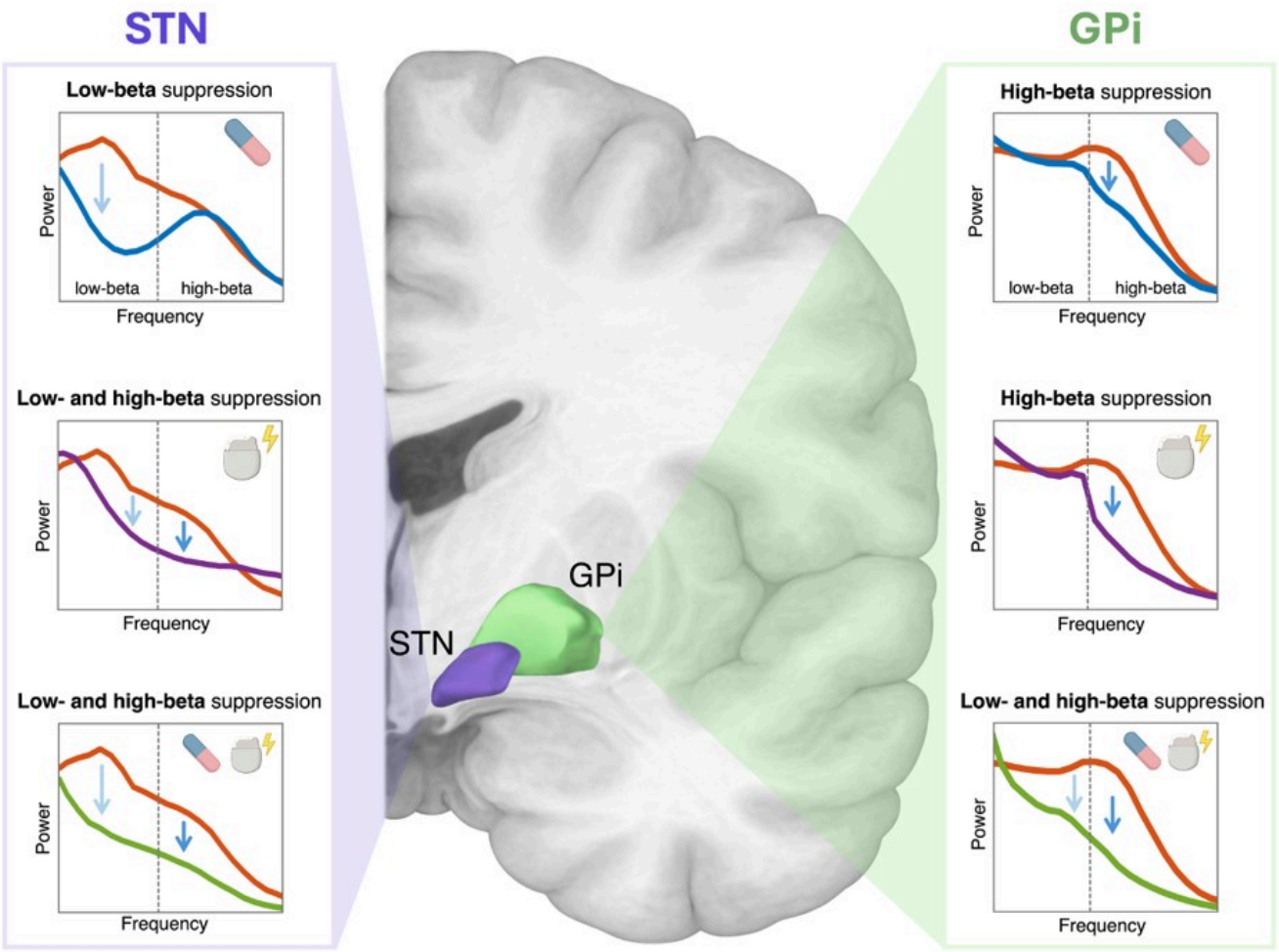


Figure 6

Summary of differential therapeutic effects between Subthalamic Nucleus (STN) and Globus Pallidus internus (GPi). The central panel shows the anatomical locations of the Subthalamic Nucleus (STN, purple) and Globus Pallidus internus (GPi, green), rendered using Lead-DBS. Surrounding panels illustrate spectral modulation in the low- and high-beta ranges under DBS and/or L-Dopa in the STN (left) and GPi (right). Red traces represent the baseline condition (M-OFF/S-OFF), while colored traces indicate power spectra following L-Dopa intake (M-ON/S-OFF, blue), DBS activation (M-OFF/S-ON, purple) and combined L-Dopa and DBS (M-ON/S-ON, green). Blue arrows indicate beta suppression between conditions and dashed vertical lines separate low- and high-beta frequency ranges. L-Dopa preferentially reduces low-beta activity in the STN and higher beta activity in the GPi. DBS produces broadband beta suppression in the STN, whereas in the GPi it predominantly suppresses higher beta frequencies. In both targets, combined L-Dopa and DBS result in broadband beta suppression.

Supplementary Files

This is a list of supplementary files associated with this preprint. Click to download.

- DOnofrioetal.SupplementaryInformation.pdf